# The FY-3D Global Active Fire product: Principle, Methodology and Validation

**Jie Chen， Wei Zheng， Cheng Liu**

**2022/11/17**

National Satellite Meteorological Center

China Meteorological Administration

**E-mail: chenjie@cma.gov.cn**

# Major Contents

1. Introduction of satellite fire monitoring
2. Theory and method for wild fire detection
3. Validation of FY-3D fire product
4. Application examples of fire monitoring

# Major Contents

1. Introduction of satellite fire monitoring
2. Theory and method for wild fire detection
3. Validation of FY-3D fire product
4. Application examples of fire monitoring


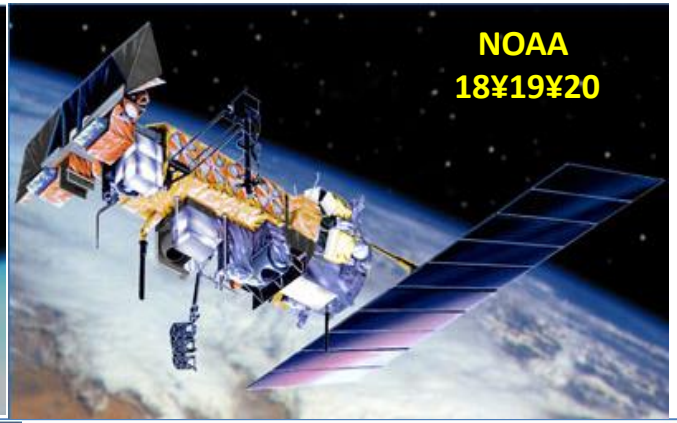


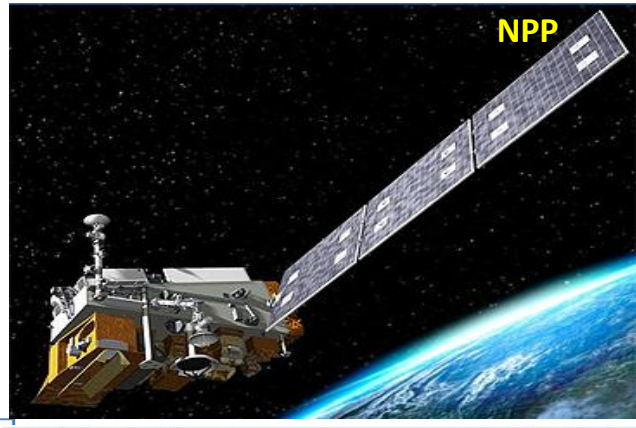


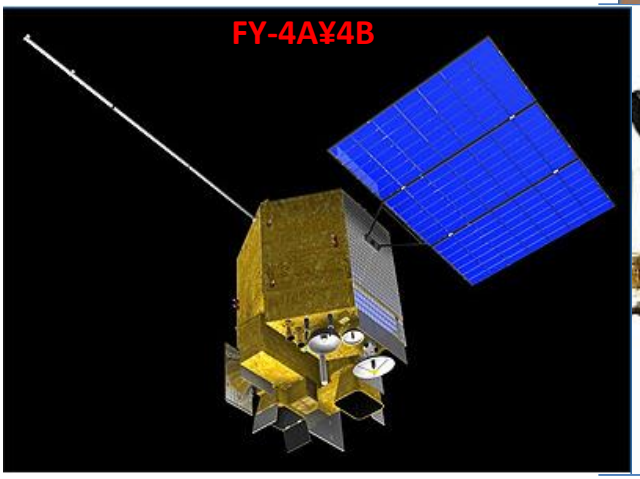



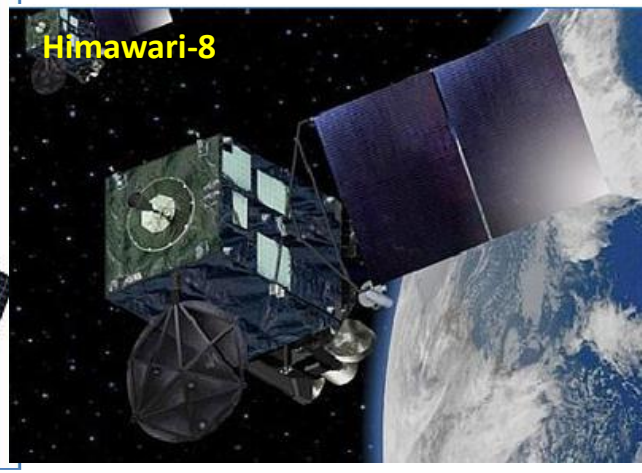


| Satellite | Series | Observation frequency | Resolution（m） | Sensitivity（m²） |
|---|---|---|---|---|
| FY-3C | Polar orbit | 2 | 1000 | 70 |
| FY-3D | | 2 | 1000 | 70 |
| FY-3E | | 2 | 1000 | 70 |
| NPP | | 2 | 375/750 | 15/45 |
| NOAA-20 | | 2 | 375/750 | 15/45 |
| TERRA | | 2 | 1000 | 60 |
| AQUA | | 2 | 1000 | 60 |
| FY-4A | Geostationary | >200 | 2000 | 250 |
| FY-4B | | 96 | 2000 | 200 |
| Himawari-8 | | 144 | 2000 | 200 |

Table. Parameters of FY-3D/MERSI compared with MODIS/Aqua in fire monitoring

| Channel | | Wavelength/μm | | Waveband | | Resolution/km | |
|---|---|---|---|---|---|---|---|
| MERSI | MODIS | MERSI | MODIS | MERSI | MODIS | MERSI | MODIS |
| 1 | 3 | 0.470 | 0.469 | Visible light | | 0.25 | 0.50 |
| 2 | 4 | 0.550 | 0.555 | Visible light | | 0.25 | 0.50 |
| 3 | 1 | 0.650 | 0.645 | Visible light | | 0.25 | 0.25 |
| 4 | 2 | 0.865 | 0.859 | Near infrared | | 0.25 | 0.25 |
| 20 | 20 | 3.800 | 3.750 | Medium infrared | | 1.00 | 1.00 |
| 21 | 23 | 4.050 | 4.050 | Medium infrared | | 1.00 | 1.00 |
| 24 | 31 | 10.800 | 11.030 | Far infrared | | 0.25 | 1.00 |
| 25 | 32 | 12.000 | 12.020 | Far infrared | | 0.25 | 1.00 |

# 1. Introduction of satellite fire monitoring

## Characteristics of spatial distribution

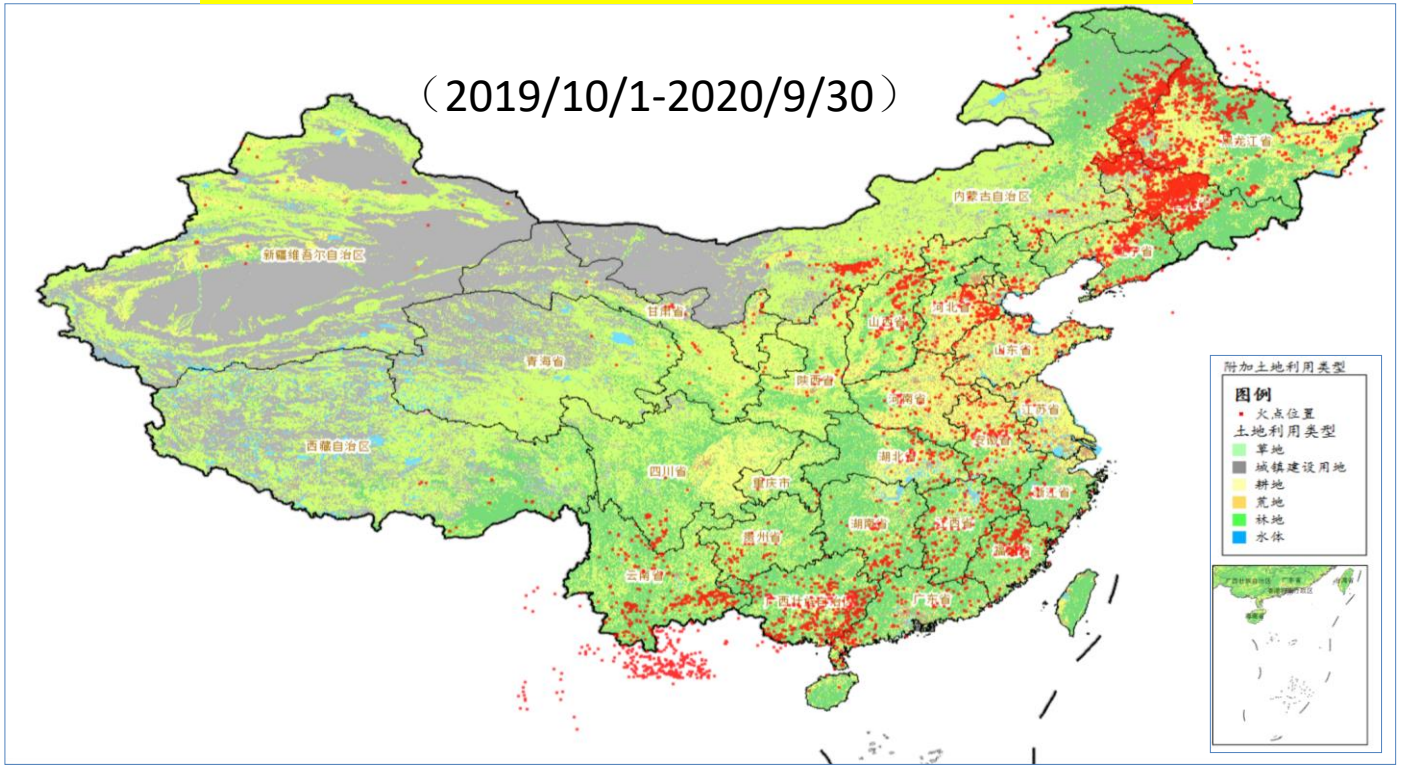


The fires mainly occurred in Northeast ,South, Southwest and North China, such as JiLin, GuangXi, YunNan and other provinces.

# Major Contents

1. Introduction of satellite fire monitoring
2. Theory and method for wild fire detection
3. Validation of FY-3D fire product
4. Application examples of fire monitoring

# 2. Theory and method for wild fire detection

The Sensitivity of satellite infrared channel.

According to Wine's law of radiation :

$$\lambda_m * T = 2897.8 \ (\mu_m \ K)$$

when temperature of blackbody goes up, the wavelength of peak radiation moves to shorter waves of the spectrum.

The temperature of forest fire and grass land fire is around 600K to 1200K, and their wavelength of peak radiation is around **2.5 to 4.5** $\mu_m$. The temperature of ground surface is about 300K, the wavelength of peak radiation is about 10 $\mu_m$.

# 2. Theory and method for wild fire detection

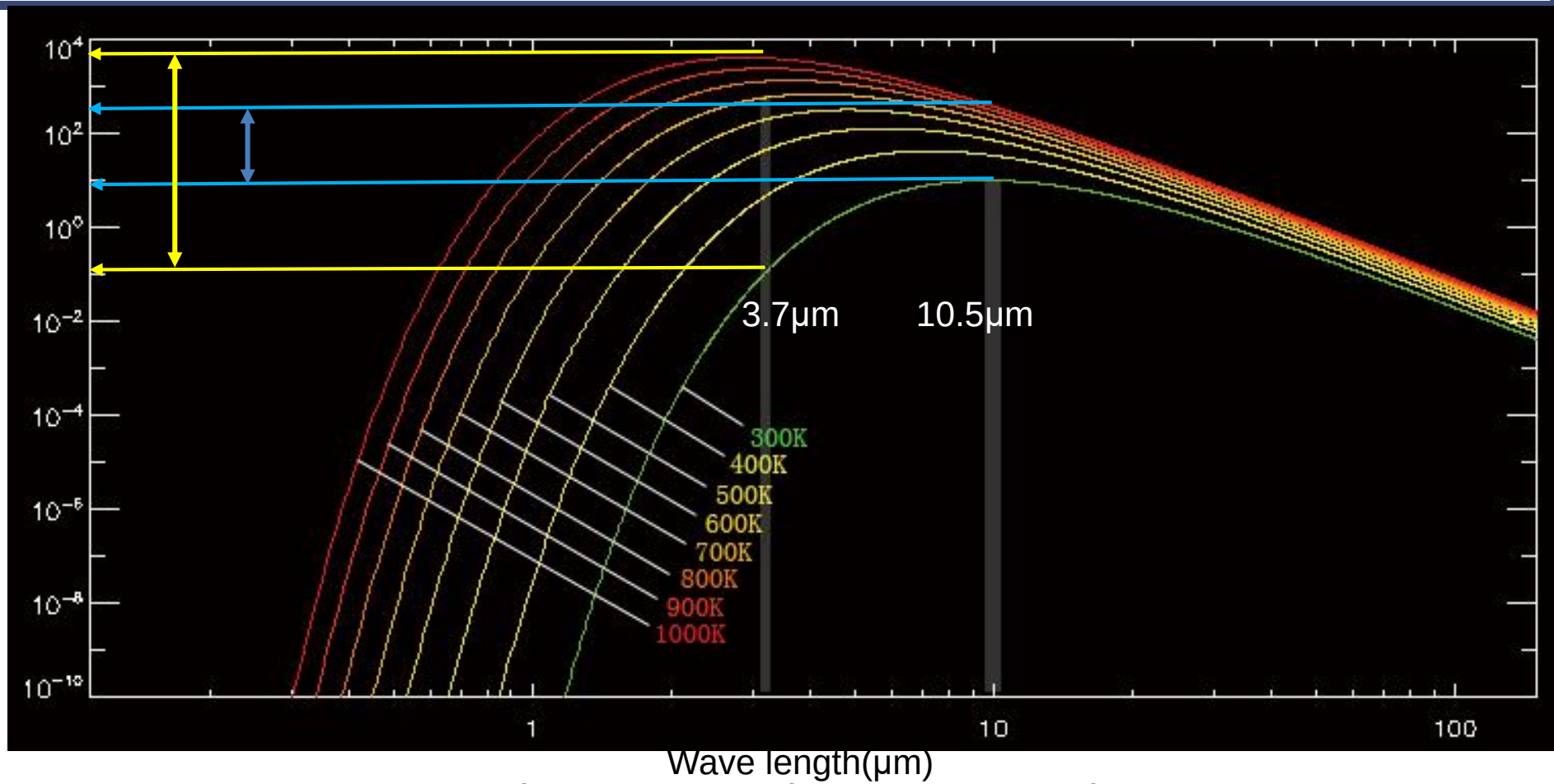


Figure. Planck radiances function curve for temperatures from 300K to 1000K. For a given increase in temperature, the increase in area under the channel 3 segments of the curves is much greater than under the channel 4 segments.

# 2. Theory and method for wild fire detection

## (1)Cloud mask

| number | conditions |
|---|---|
| 1 | $T_{Mir} - T_{far1} < 4K$ |
| 2 | $T_{Mir} - T_{far1} > 20K$ & $T_{Mir} < 285K$ \| $T_{far1} < 280K$ |
| 3 | $R_{Vis} > 0.28$ |
| 4 | $T_{far1} < 265K$ |
| 5 | $T_{Mir} < 270K$ & $T_{far1} - T_{far2} < 4K$ |
| 6 | $T_{far1} < 270K$ & $T_{far1} - T_{far2} > 60K$ |
| 7 | $T_{Mir} < 320K$ & $T_{Mir} < T_{Mir\_TH}$ |
| 8 | $R_{Vis} > 0.28$ $T_{Mir} < 320K$ |

## (2)Fire pixels identification

1) $T_{3.9} > T_{3.9bg} + n_1 \times \delta T_{3.9bg}$

2) $\Delta T_{3.9\_11} > \Delta T_{3.9bg\_11bg} + n_2 \times \delta T_{3.9bg\_11bg}$

## (3)Sub-pixel fire spot area estimate

$$N_{imix} = P * N_{ihi} + (1 - P) * N_{ibg}$$
$$= P * \frac{C_1 V_i^3}{e^{\frac{C_2 V_i}{T_{hi}}} - 1} + (1 - P) * \frac{C_1 V_i^3}{e^{\frac{C_2 V_i}{T_{bg}}} - 1}$$

## (4)Calculation fire radiation power

$$FRP = P * S_{\lambda,\varphi} * \sigma T^4$$

# 2. Theory and method for wild fire detection

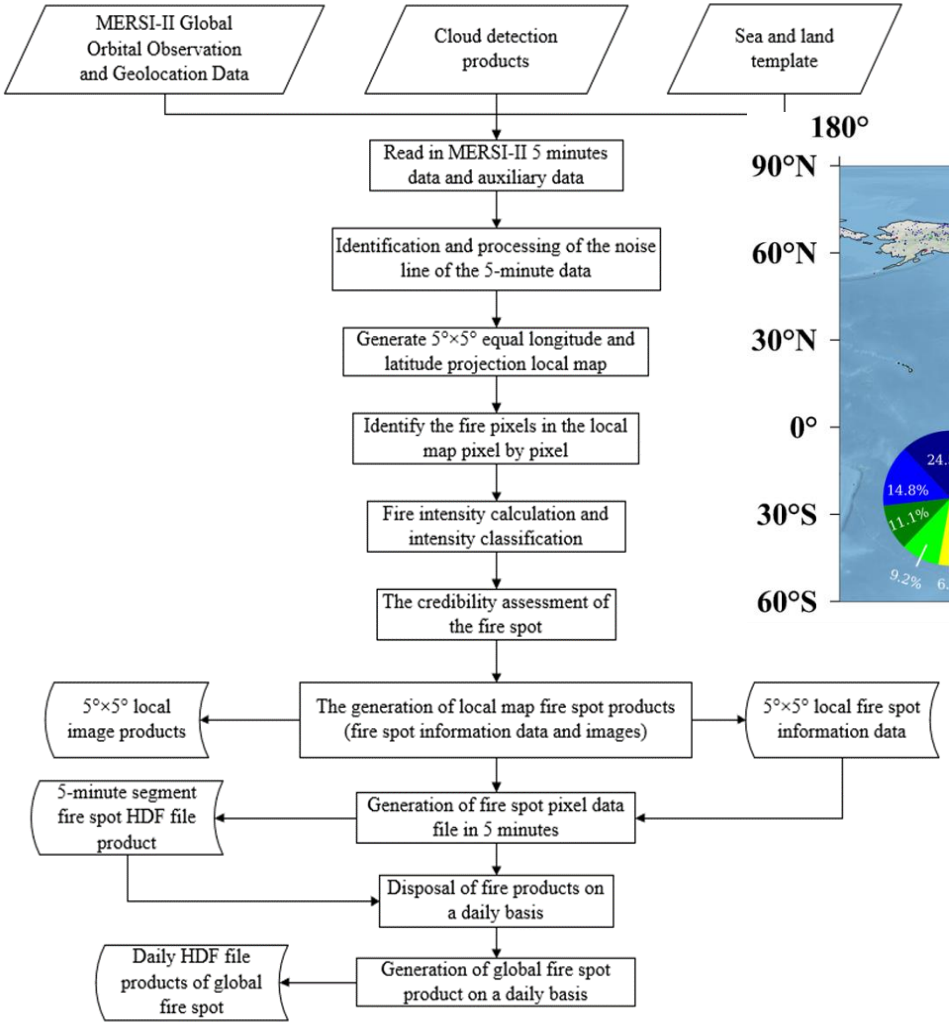


General flow chart for generating FY-3D fire spot products

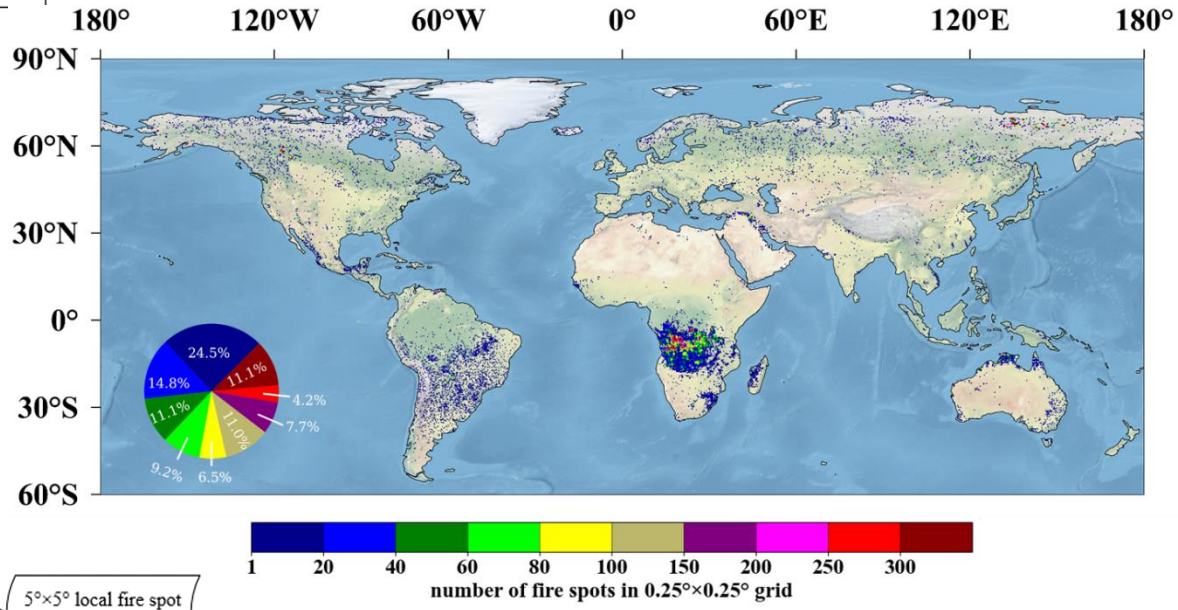


Density map of global fire spots based on FY-3D (2019-06)

# Major Contents

1. Introduction of satellite fire monitoring
2. Theory and method for wild fire detection
3. Validation of FY-3D fire product
4. Application examples of fire monitoring

# 3. Validation of FY-3D fire product

## Verification methods

$$\sqrt{(lat1 - lat2)^2 + (long1 - long2)^2} \leq 0.02°$$

## (1) Assessment of FY-3D fire products based on visual interpretation

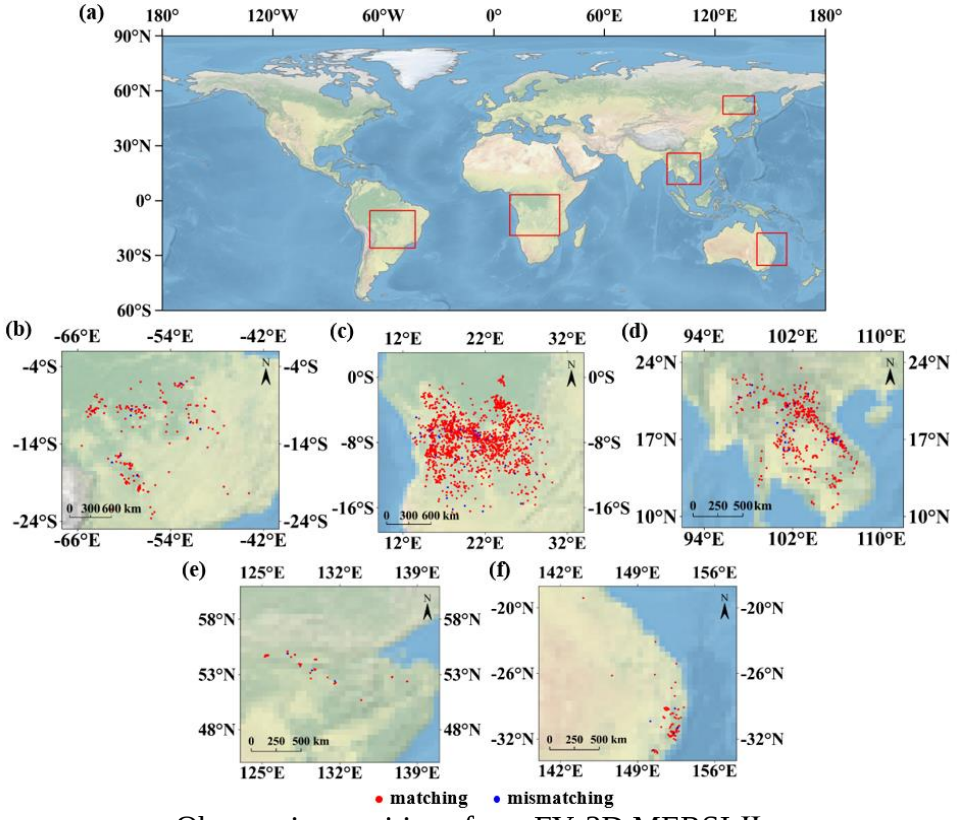


Observation positions from FY-3D MERSI-II

| Region | GFR-based fire spots | Not match | Accuracy (%) |
|---|---|---|---|
| South-central Africa | 1429 | 77 | 94.6 |
| East-central South America | 204 | 12 | 94.1 |
| Siberia | 32 | 3 | 90.6 |
| Australia | 85 | 7 | 91.8 |
| Indo-China Peninsula | 438 | 32 | 92.7 |
| Overall | 2188 | 131 | 94.0 |

Clean sky

# 3. Validation of FY-3D fire product

## (2) Cross-validation between FY-3D and MODIS global fire products

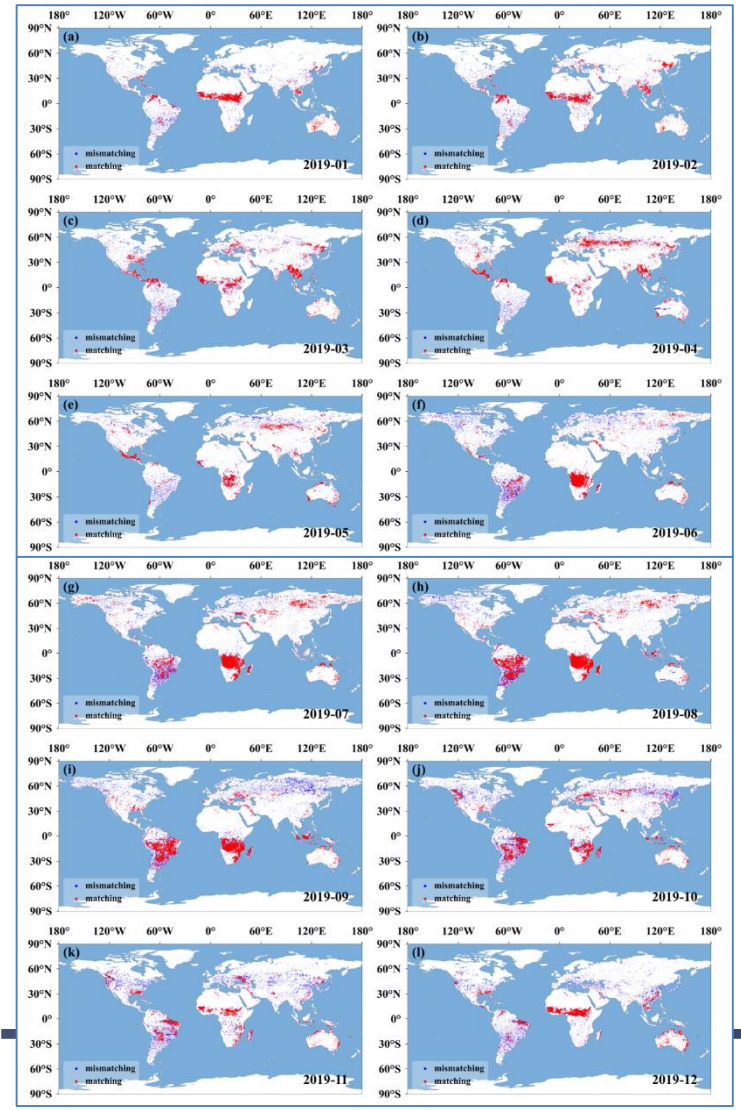


1) Validation in different months

| Time | Match | Mismatch | Total | Consistence (%) |
|---|---|---|---|---|
| 201901 | 70799 | 14188 | 84987 | 83 |
| 201902 | 66849 | 14717 | 81566 | 82 |
| 201903 | 105176 | 22576 | 127752 | 82 |
| 201904 | 94474 | 39250 | 133724 | 71 |
| 201905 | 75703 | 17135 | 92838 | 82 |
| 201906 | 174587 | 33862 | 208449 | 84 |
| 201907 | 362108 | 39683 | 401791 | 90 |
| 201908 | 315182 | 51627 | 366809 | 86 |
| 201909 | 226363 | 47607 | 273970 | 83 |
| 201910 | 115975 | 33956 | 149931 | 77 |
| 201911 | 102240 | 27732 | 129972 | 79 |
| 201912 | 157464 | 28461 | 185925 | 85 |
| Total | 1866920 | 370794 | 2237714 | 83.4 |

# 3. Validation of FY-3D fire product

## 2) Validation on different underlying surfaces

| ID | Jan | Feb | Mar | Apr | May | Jun | Jul | Aug | Sep | Oct | Nov | Dec |
|---|---|---|---|---|---|---|---|---|---|---|---|---|
| 11 | 50 | 76 | 86 | 81 | 68 | 66 | 54 | 77 | 80 | 85 | 73 | 56 |
| 14 | 64 | 57 | 73 | 81 | 71 | 64 | 56 | 79 | 85 | 73 | 73 | 57 |
| 20 | 72 | 67 | 78 | 83 | 78 | 68 | 64 | 81 | 87 | 73 | 77 | 79 |
| 30 | 65 | 63 | 77 | 84 | 82 | 84 | 84 | 77 | 83 | 83 | 79 | 75 |
| 40 | 94 | 88 | 75 | 84 | 85 | 74 | 72 | 76 | 83 | 83 | 80 | 82 |
| 50 | 61 | 72 | 82 | 88 | (87 | 86 | 85 | 71 | 81 | 79 | 80 | 66 |
| 60 | 90 | 85 | 75 | 87 | 86 | 89 | 89 | 82 | 82 | 79 | 86 | 89 |
| 70 | 56 | 79 | 80 | 87 | 82 | 90 | 73 | 86 | 82 | 77 | 49 | 66 |
| 90 | 35 | 57 | 62 | 56 | 97 | 98 | 91 | 85 | 64 | 72 | 82 | 56 |
| 100 | 49 | 59 | 71 | 59 | 82 | 93 | 87 | 92 | 70 | 75 | 70 | 66 |
| 110 | 84 | 84 | 73 | 67 | 80 | 92 | 84 | 88 | 84 | 86 | 86 | 81 |
| 120 | 83 | 81 | 77 | 65 | 86 | 93 | 86 | 85 | 51 | 84 | 88 | 87 |
| 130 | 87 | 85 | 85 | 87 | 84 | 86 | 85 | 76 | 85 | 87 | 82 | 84 |
| 140 | 76 | 66 | 78 | 80 | 76 | 85 | 78 | 80 | 26 | 82 | 87 | 87 |
| 150 | 77 | 71 | 77 | 60 | 81 | 87 | 58 | 71 | 24 | 75 | 88 | 92 |

| ID | Definition of underlying surfaces |
|---|---|
| 11 | Post-flooding or irrigated croplands (or aquatic) |
| 14 | Rainfed croplands |
| 20 | Mosaic cropland (50-70%) / vegetation (grassland/shrubland/forest) (20-50%) |
| 30 | Mosaic vegetation (grassland/shrubland/forest) (50-70%) / cropland (20-50%) |
| 40 | Closed to open (>15%) broadleaved evergreen or semi-deciduous forest (>5m) |
| 50 | Closed (>40%) broadleaved deciduous forest (>5m) |
| 60 | Open (15-40%) broadleaved deciduous forest/woodland (>5m) |
| 70 | Closed (>40%) needleleaved evergreen forest (>5m) |
| 90 | Open (15-40%) needleleaved deciduous or evergreen forest (>5m) |
| 100 | Closed to open (>15%) mixed broadleaved and needleleaved forest (>5m) |
| 110 | Mosaic forest or shrubland (50-70%) / grassland (20-50%) |
| 120 | Mosaic grassland (50-70%) / forest or shrubland (20-50%) |
| 130 | Closed to open (>15%) (broadleaved or needleleaved, evergreen or deciduous) shrubland (<5m) |
| 140 | Closed to open (>15%) herbaceous vegetation (grassland, savannas or lichens/mosses) |
| 150 | Sparse (<15%) vegetation |

**Depending on the combustible vegetation!!!**

When the underlying surface is the open coniferous and deciduous forest or evergreen forest, the consistence is the highest, at 93%. In addition, according to the classification of underlying surfaces, the fire spot identification shows high consistence when the underlying surface is the forest.

The low consistence between FY-3D and MODIS fire products was observed for underlying surface cropland and sparse vegetable. These surfaces were all covered by sparse or unstable vegetation, the fire on which can last for a relatively short period. Meanwhile, the observation time lag between FY-3D and MODIS was larger than 30 minutes. Therefore, the consistence of FY-3D and MODIS fire products on these surface types was lower than other surface types.

# 3. Validation of FY-3D fire product

3) Validation in different regions

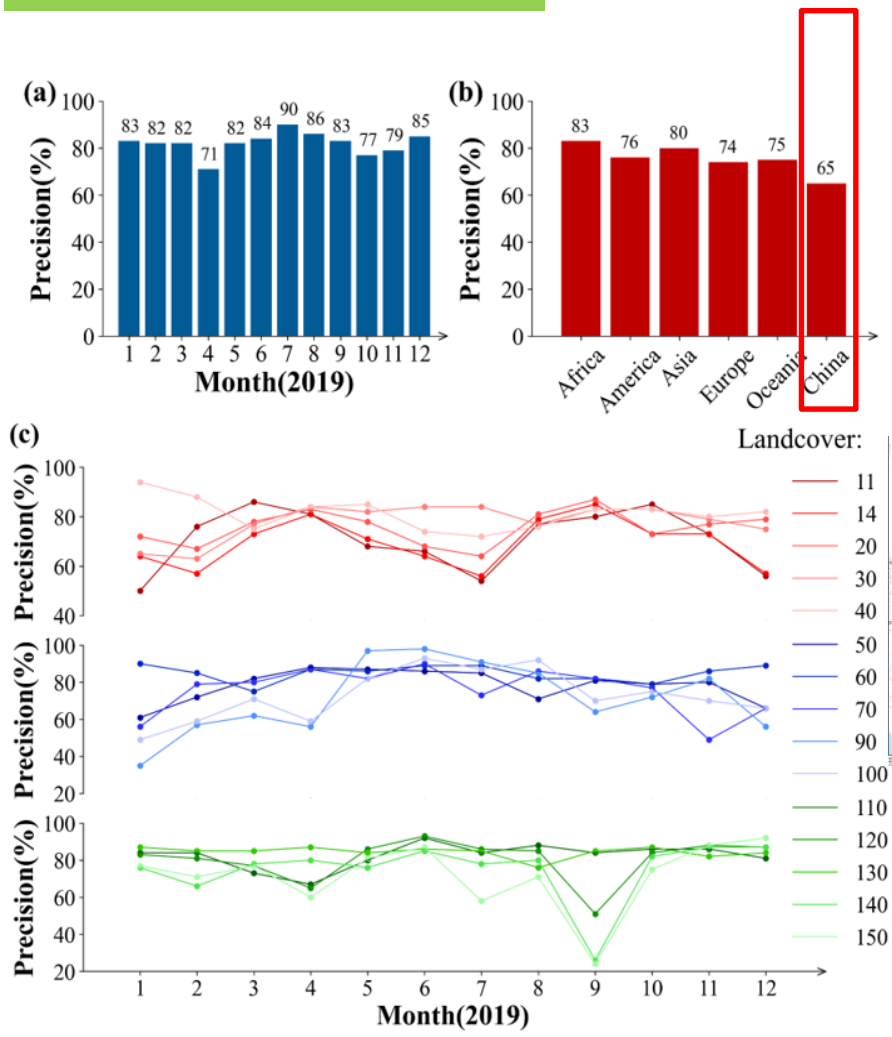


**The global monitoring area is divided into Africa, America, Asia, Europe, and Oceania. The verification demonstrates the results with the highest consistence (over 80%) are found in Africa and Asia, and those in America, Europe, and Oceania show the consistence over 70%.**

**China's regional consistency of results in China is lower than other continents, only 65%.**

Interference factors

**Specular reflection**

**thermal anomaly**

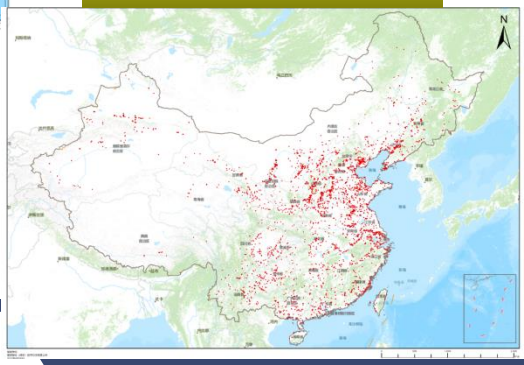

# Major Contents

1. Introduction of satellite fire monitoring
2. Theory and method for wild fire detection
3. Validation of FY-3D fire product
4. Application examples of fire monitoring

# 4. Application examples of fire monitoring


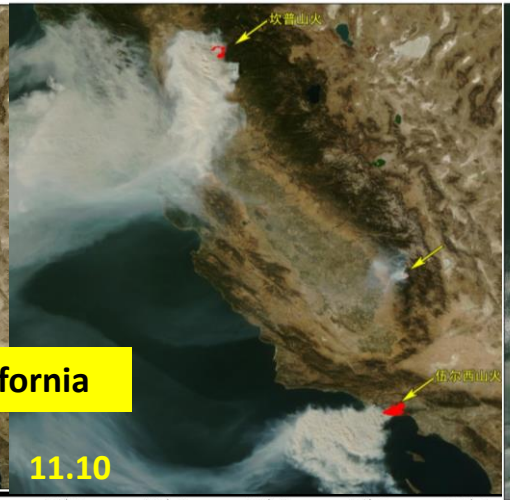


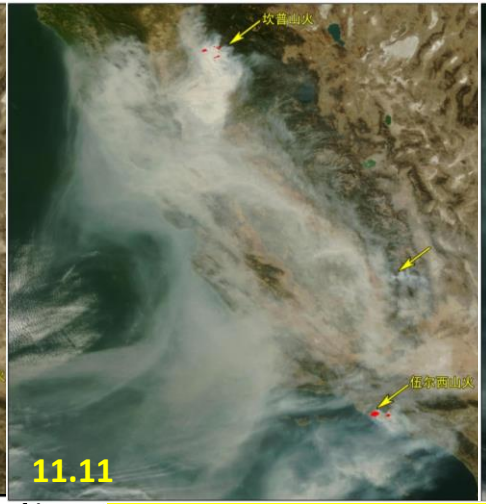


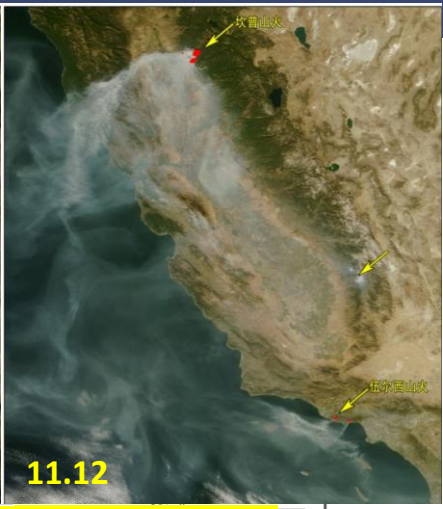


FY-3D Monitor wildfires in California

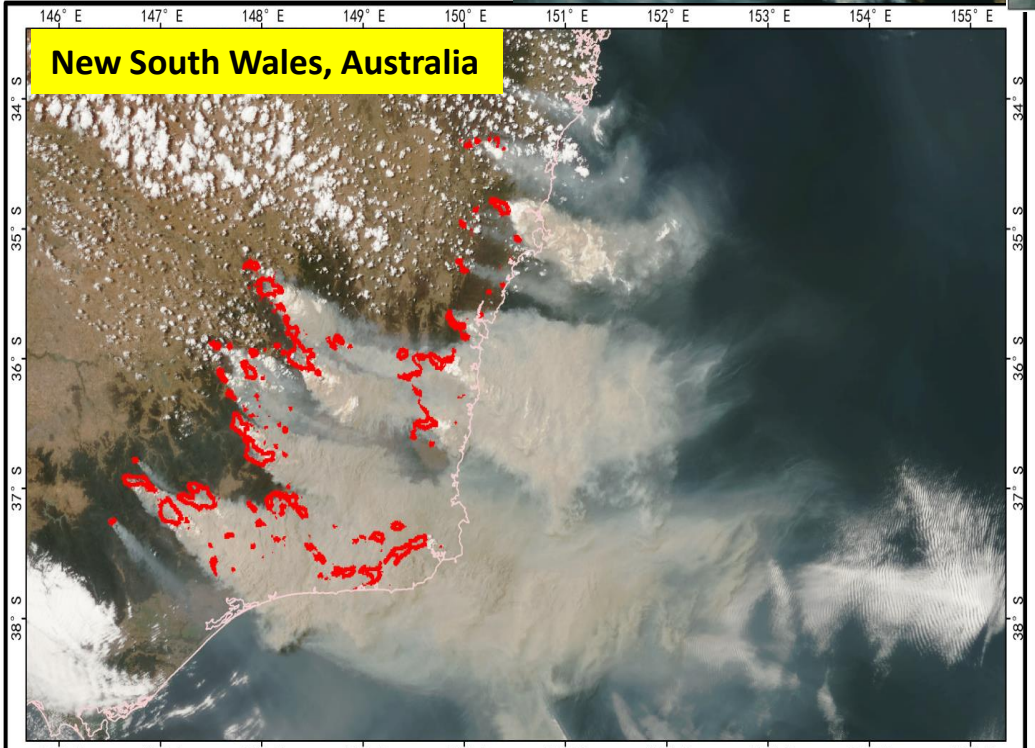


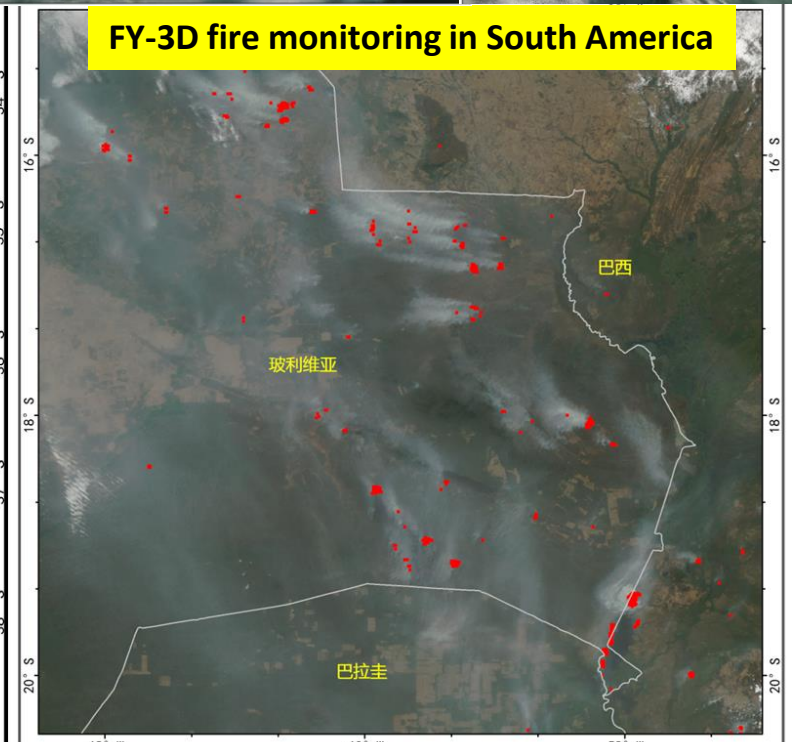

# 4. Application examples of fire monitoring

FY-3D fire monitoring in The Mediterranean Sea compare 2021 to 2020

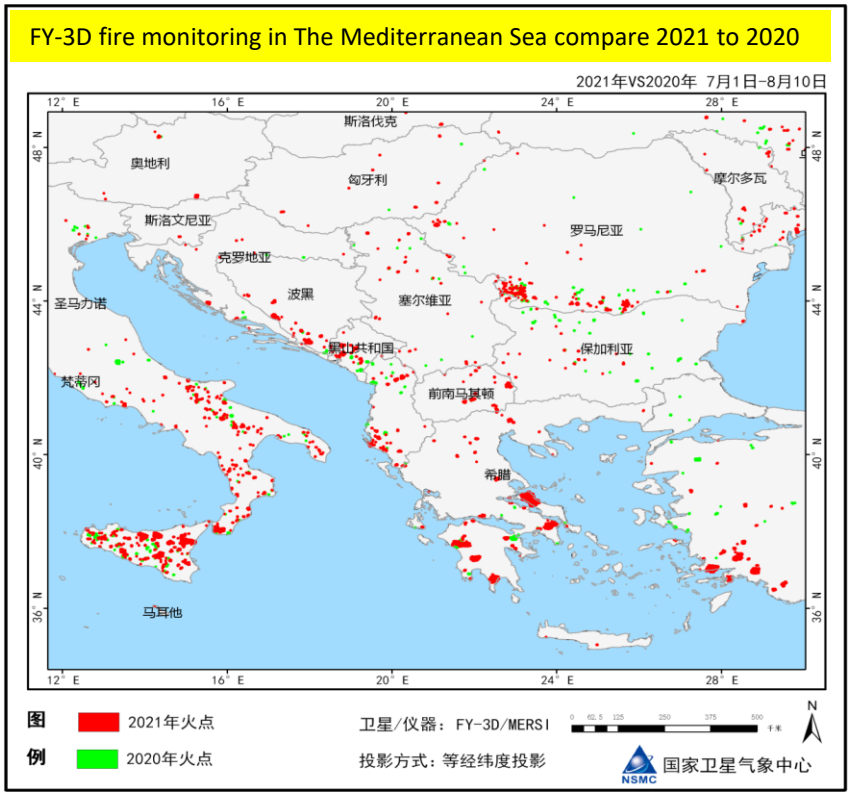


FY-3 fire monitoring in Arctic Circle compare 2018 to 2017

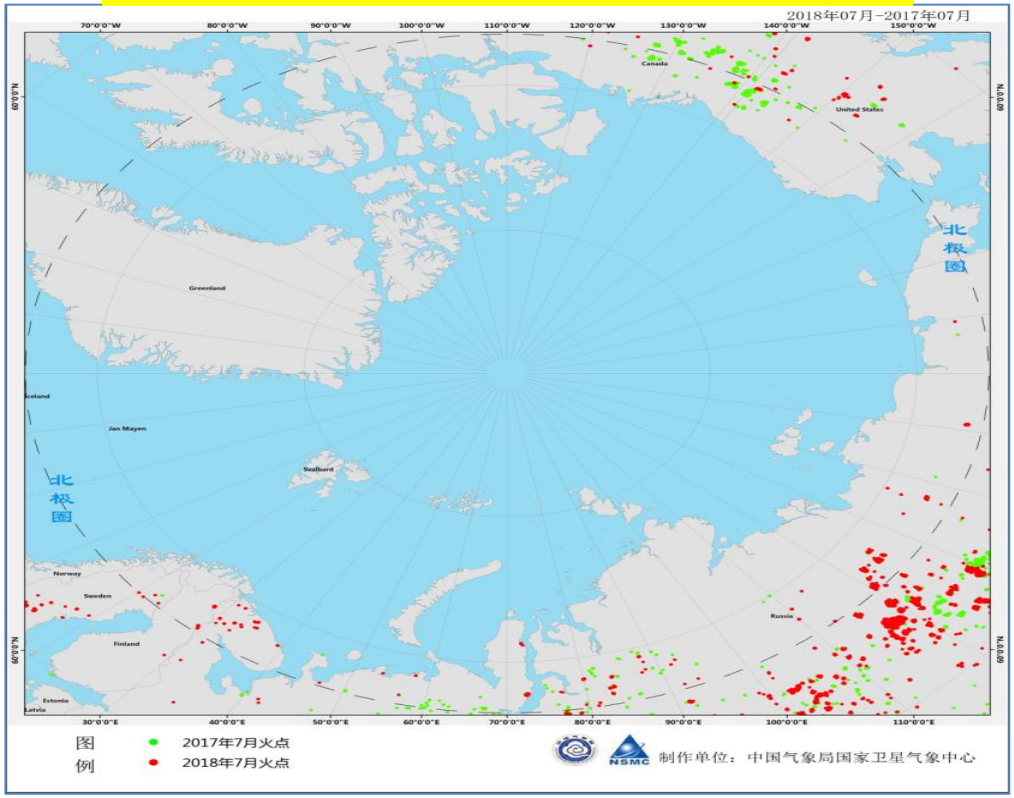

# 4. Application examples of fire monitoring

## Multi-source satellites in fire monitoring

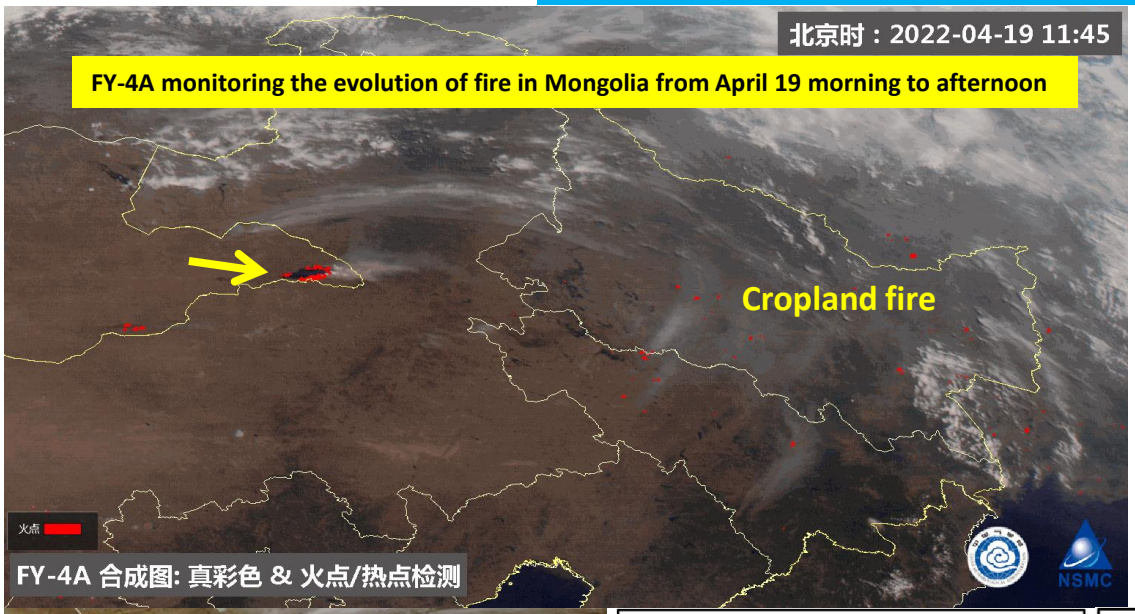


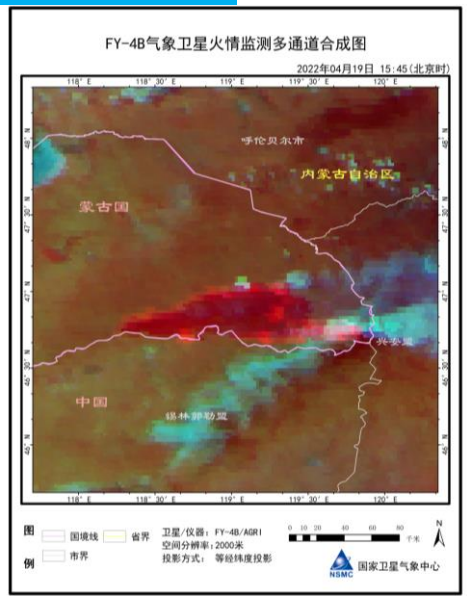


FY-4B monitoring the fire
2022/4/19 15:45

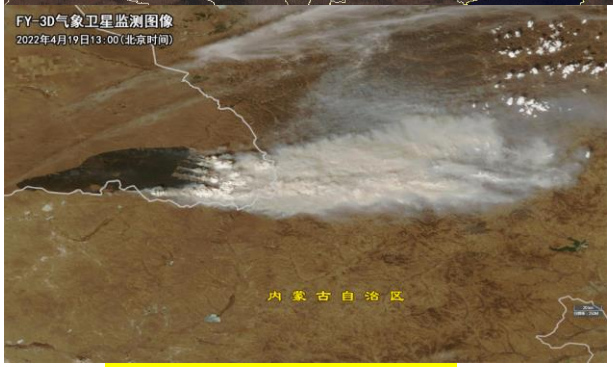


FY-3D monitoring the fire area
2022/4/19 13:00

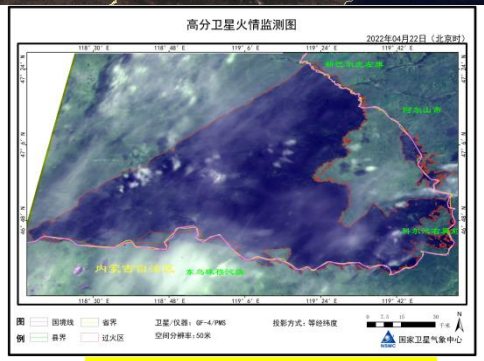


GF-4 monitoring the fire area
2022/4/22

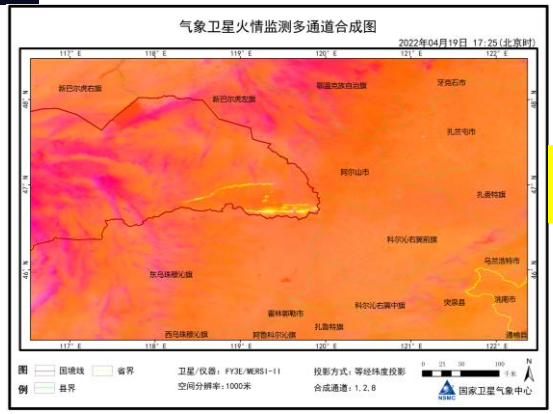


FY-3E monitoring the fire
2022/4/19 17:25

Earth Syst. Sci. Data, 14, 3489–3508, 2022
https://doi.org/10.5194/essd-14-3489-2022


Open Access Earth System Science Data

# The Fengyun-3D (FY-3D) global active fire product: principle, methodology and validation

Jie Chen[1,2,★], Qi Yao[3,★], Ziyue Chen[3], Manchun Li[4], Zhaozhan Hao[5], Cheng Liu[1,2], Wei Zheng[1,2], Miaoqing Xu[3], Xiao Chen[3], Jing Yang[3], Qiancheng Lv[3], and Bingbo Gao[5]

## Viewed (geographical distribution)

Show all | Final revised paper only | Preprint only

**Total article views: 1,160** (including HTML, PDF, and XML)

Thereof 1,160 with geography defined and 0 with unknown origin.

| Country | # | Views | % |
|---|---|---|---|
| China | 1 | 380 | 32 |
| United States of America | 2 | 248 | 21 |
| Germany | 3 | 88 | 7 |
| France | 4 | 37 | 3 |
| undefined | 5 | 35 | 3 |


FY-3D fire product download address:
http://data.nsmc.org.cn/PortalSite/Data/Satellite.aspx?currentculture=en-US


**The End**

*Thanks for your attention!*